

# Toughening and Compatibilization of Polyphenylene Sulfide/Nylon 66 Blends with SEBS and Maleic Anhydride Grafted SEBS Triblock Copolymers

Weihua Tang,<sup>1,2</sup> Xiaoyi Hu,<sup>1</sup> Jian Tang,<sup>1</sup> Riguang Jin<sup>1</sup>

<sup>1</sup>School of Materials Science and Engineering, Beijing University of Chemical Technology, Beijing 100029, People's Republic of China

<sup>2</sup>Institute of Materials Research and Engineering, Singapore 117602, Singapore

Received 8 January 2007; accepted 17 May 2007

DOI 10.1002/app.26832

Published online 30 July 2007 in Wiley InterScience (www.interscience.wiley.com).

**ABSTRACT:** In this study, styrene-*b*-ethylene/butylene-*b*-styrene triblock copolymer (SEBS) and maleic anhydride grafted SEBS (SEBS-*g*-MA) were used as compatibilizers for the blends of polyphenylene sulfide/nylon 66 (PPS/PA66). The mechanical properties, including impact and tensile properties and morphology of the blends, were investigated by mechanical properties measurements and scanning electron microscopy. Impact measurements indicated that the impact strength of the blends increases slowly with elastomer (SEBS and SEBS-*g*-MA) content upto 20 wt %; thereafter, it increases sharply with increasing elastomer content. The impact energy of the elastomer-compatible PPS/PA66 blends exceeded that of pure nylon 66, implying that the nylon 66 can be further toughened by the incorporation

of brittle PPS minor phase in the presence of SEBS or SEBS-*g*-MA. The compatibilization efficiency of SEBS-*g*-MA for nylon-rich PPS/PA66 was found to be higher than SEBS due to the *in situ* forming SEBS interphase between PPS and nylon 66. The correlation between the impact property and morphology of the SEBS-*g*-MA compatibilized PPS/PA66 blends is discussed. The excellent impact strength of the nylon-rich blends resulted from shield yielding of the matrix. © 2007 Wiley Periodicals, Inc. *J Appl Polym Sci* 106: 2648–2655, 2007

**Key words:** polyphenylene sulfide; nylon 66; SEBS; maleic anhydride grafted SEBS; toughening; compatibilization; blends; morphology

## INTRODUCTION

The commercial significance of polyphenylene sulfide (PPS) and nylon (PA) are well known and confirmed by their tremendous engineering applications. PPS is widely used in injection-molded components with complicated shapes for various engineering components because of its features such as excellent thermal stability, chemical resistance, flame resistance and precise moldability, as well as high stiffness and modulus.<sup>1–3</sup> However, PPS suffers the disadvantage of low toughness because of its rigid structure.<sup>4,5</sup> Nylon 66 (PA66) is an excellent high-performance engineering thermoplastic with many desirable characteristics, including good mechanical properties (both strength and toughness), thermal stability, chemical resistance, and melt processability.<sup>6</sup> If one would like to improve the toughness of PPS and conversely improve the melt strength of PA66, it would be highly desired to blend PPS with PA66, which should provide useful polymer alloys with the balanced properties and advantages from

individual components. However, no such studies have been reported on the toughened PPS/PA66 system; only several reports on the formulation of elastomer-toughened PPS blends such as PPS/olefinic elastomer, PPS/ABS, and PPS/SEBS blends.<sup>4,7–10</sup> Kubo et al.<sup>4,7</sup> made an advance in PPS toughening by using diphenylmethane diisocyanate (MDI) to activate the reactivity of the PPS end-group via extrusion. Reactive processing of the MDI-treated PPS with an olefinic elastomer containing a functional group such as carboxylic acid anhydride gave toughened PPS. The elastomer was finely dispersed in the matrix. It is generally known that in those elastomer toughened polymer blends, the rubbery domains act as stress concentrators when subject to external forces. Polymer alloys are toughened because of the relaxation of stress concentration, resulting in the formation of many voids in the elastomer particles with low cohesive force and the development of crazes at the peripheries of rubbery domains.<sup>11,12</sup> The efficiency of improvement in toughness depends on both the strength of craze and the degree of relaxation of stress concentration.<sup>13</sup> A disadvantage of this modification with low-modulus elastomer is the sharp decrease in tensile strength of the blends.<sup>4,7–10,14</sup> This invites the investigation of introducing ductile thermoplastics such as

Correspondence to: W. Tang (wh-tang@imre.a-star.edu.sg).

TABLE I  
Characteristics of the Virgin Materials Used in This Study

Polymer	Form	Manufacturer	Trade name	$M_w$ ( $\times 10^{-3}$ g mol)	Melting point ( $^{\circ}$ C)	Density (g/cm <sup>3</sup> )
PPS	Powder	Sichuan Deyang Sci. & Techn. Co., China	–	48	286	1.34
PA66	Pellet	Du Pont, USA	Zytel 101L	20	262	1.14
SEBS	Pellet	Shell, USA	Kraton G1652	–	–	0.91
SEBS- <i>g</i> -MA	Pellet	Shell, USA	Kraton FG1901X	–	–	0.91

S, styrene; EB, ethylene butylene.

HDPE, PC, and nylon 6 into the elastomer-toughened polymer blends.<sup>14,15</sup> The recent research involving PPS/PA66 blends was mainly focused on their tribological properties when filling with polytetrafluoroethylene (PTFE) and glass fibre.<sup>16,17</sup>

In this article, a styrene-*b*-ethylene/*b*-butylene-*b*-styrene triblock copolymer (SEBS) and maleic anhydride grafted SEBS (SEBS-*g*-MA) were employed as impact modifiers. Systematical examination of the compatibilization efficiency of SEBS and SEBS-*g*-MA on PPS/PA66 blends was carried out by investigating mechanical properties, including tensile and impact ones, as well as morphology of fracture surfaces of the toughened blends.

## EXPERIMENTAL

### Materials

The materials used in this study are a linear type PPS and conventional nylon 66, SEBS, and SEBS-*g*-MA. Characteristics of these virgin materials are listed in Table I. SEBS (Kraton G 1652), containing 29 wt % styrene, had a number-average molecular weight of 7000 in polystyrene block and 37,500 in the polyolefin blocks. Containing 29 wt % styrene and grafted with 1.84 wt % maleic anhydride, SEBS-*g*-MA (Kraton FG1901X) had a number average-molecular weight of 7500 for the PS block and 35,000 for the center EB block.

### Processing

Prior to blending, all components were dried in an oven overnight (nylon 66, SEBS, and SEBS-*g*-MA at 60 $^{\circ}$ C, whereas PPS at 120 $^{\circ}$ C) and dry-blended according to the desired recipe for PPS/PA66, PPS/PA66/SEBS, and PPS/PA66/SEBS-*g*-MA blends. Further, they were extruded in a co-rotating twin-screw extruder ( $L/D = 30$ ) operated at 90 rpm. The processing temperature from feed to die was 250, 270, 280, 300, and 280 $^{\circ}$ C for complete melt mixing. For mechanical property evaluation, the pellets obtained were injection-molded in an injection-molding machine (SZ-160/80 NB, China) to prepare the test specimens. The dimensions of the tensile bars

and notched impact specimens corresponded to ASTM D638 and ASTM D256, respectively.

### Measurement of mechanical properties

Tensile tests were carried out using Universal Tensile Testing Machine (model 3211, Instron, UK) according to ASTM D 638-95. The crosshead jaw speed was 10 mm/min and a load cell of 5 KN capacity was used.

Izod and Charpy impact strength of the notched rectangular bars were measured using a pendulum impact testing machine (XJ-40A, Wuzhong Material Testing Machine Company, Hebei, China). During impact test, a load cell in the tup recorded the force generated in the deformed sample.

### Morphological observations

The morphological characteristics were examined by SEM (Cambridge-5250, UK). Two kinds of specimen surfaces after impact tests were observed, that is, beyond notch cryogenically-fractured surfaces and near notch impact-fractured surfaces at room temperature. All samples were coated with a thin layer of gold to increase the contrast between the matrix and the dispersed phase in the morphology study.

## RESULTS AND DISCUSSION

### Dispersion of SEBS-*g*-MA in PA66

The toughening effect of SEBS and SEBS-*g*-MA on PPS was recently studied by Hisamatsu et al.<sup>10</sup> It was confirmed that highly modified SEBS-*g*-MA (grafted with 1.8 wt % maleic acid) was dispersed finely because of high compatibility with the PPS matrix, and the toughness was improved efficiently by the release of constraint of the strain due to void formation in the elastomer particles. For SEBS and lightly modified SEBS-*g*-MA (grafted with only 0.5 wt % maleic acid) compatibilized polymer alloys, the diameter of dispersed elastomer particles was larger, and the particles were deformed into a rod-like shape and oriented along to the direction of injection flow, particularly in high content of elastomer. These

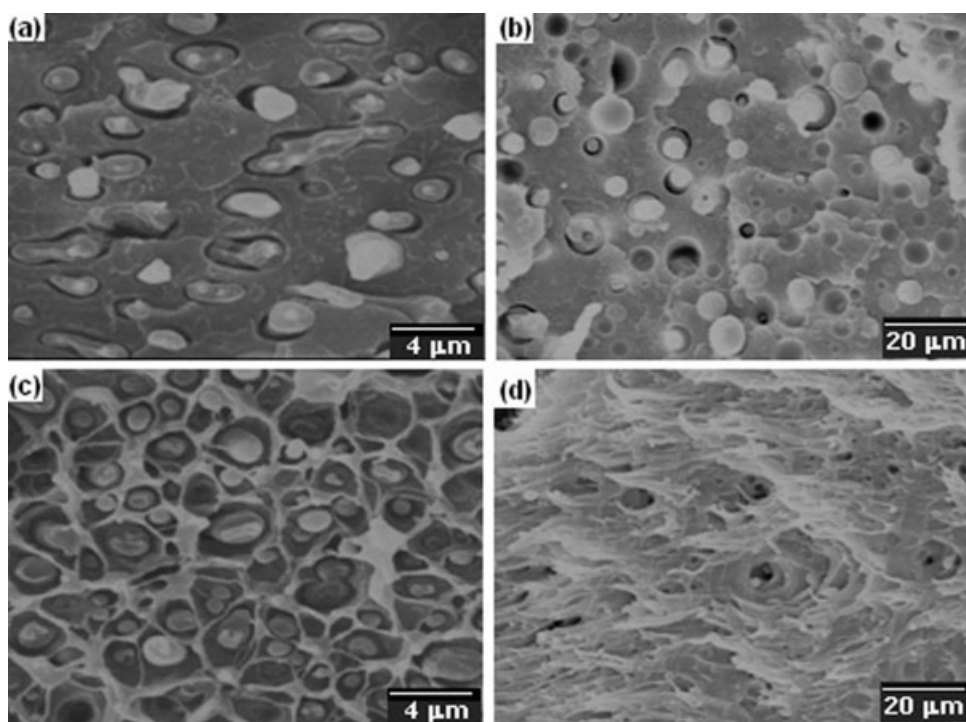


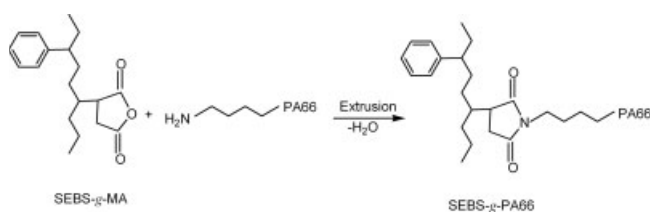
**Figure 1** SEM photomicrographs of PA66/ SEBS-g-MA blends containing: (a) 10 wt % and (b) 30 wt % SEBS-g-MA, showing the size of the elastomer. (Left panel: beyond notch, cryogenically-fractured; right panel: near notch, impact-fractured).

oriented particles were fractured easily and many cracks, which were distributed along the direction of flow, were formed. In our study of elastomer-toughened PPS/PA66 blends, a similar highly modified SEBS-g-MA was employed as impact modifier. Therefore, it is necessary to investigate the dispersion of SEBS-g-MA in PA66. Figure 1 shows photomicrographs of the fractured surfaces of PA66/SEBS-g-MA blends when containing different content of elastomer. As shown in the cryogenically-fractured surfaces [Fig. 1(a,c)], typical droplet-matrix morphology was observed for this rubber-toughened nylon blends, with SEBS-g-MA particles evenly dispersed in PA66 matrix. The average diameter of SEBS-g-MA ranges from 1 to 1.8  $\mu\text{m}$ , irrespective of its contents, which is a direct characteristic of a compatibilized blend. It is noted that some elastomer particles were elongated to give irregular shapes. As shown in the near notch morphology [Fig. 1(b,d)], some elastomer particles were pulled out from the matrix to form microvoids in the fractured surfaces. The obscure interfaces as observed from the fractograph indicate that good compatibility can be achieved between PA66 and SEBS-g-MA, which is derived from the PA66-co-SEBS-g-MA copolymer formed *in situ* during melt extrusion.<sup>18,19</sup> In this case, the maleic anhydride group of SEBS-g-MA reacts with the terminal amino group of PA66 during melt extrusion, as shown below (Scheme 1).

### Toughening effect of SEBS and SEBS-g-MA (mechanical properties)

The dependence of mechanical properties of non-compatibilized PPS/PA66 upon the content of PA66 was depicted in Figure 2 for impact properties and Figure 3 for tensile properties. In general, uncompatibilized PPS/PA66 blends displayed modified mechanical properties with both strength and ductility lower than pure nylon 66 but much higher than pure PPS. The deterioration in the mechanical properties of PA66 results from the poor interfacial adhesion due to the incompatibility between PPS and PA66. However, PPS/PA66 blends showed better stiffness and ductility than pure PPS, with the incremental addition of PA66, especially those nylon-rich blends.

To obtain useful polymer alloys, compatibilizers are therefore needed to improve the compatibiliza-



**Scheme 1** PA66-co-SEBS-g-MA copolymer formed *in situ* during melt extrusion of PA66 and SEBS-g-MA.

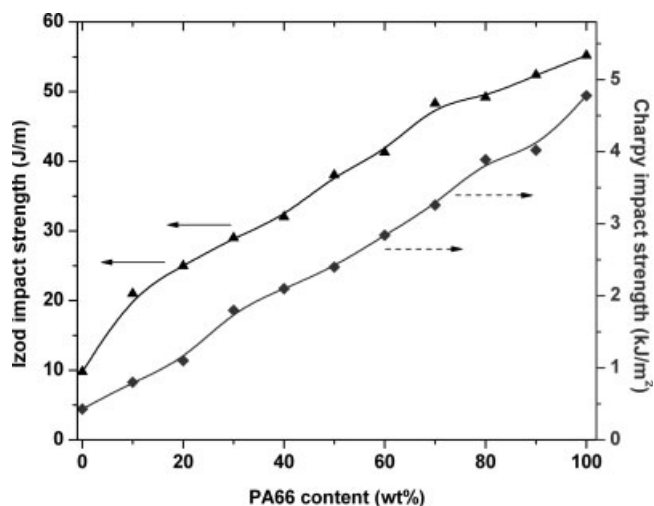


**Figure 2** Variation of Izod impact strength (▲) and Charpy impact strength (■) with PA66 content for uncompatibilized PPS/PA66 blends.

tion between PPS and PA66. Herein, SEBS and SEBS-g-MA were used as compatibilizers to investigate their compatibilization efficiency for nylon-rich PPS/PA66 (20/80) and PPS/PA66 (30/70) blends since these polymer blends presented better mechanical properties.

Figure 4 shows the Izod impact strength of SEBS and SEBS-g-MA on the selected polymer blend systems. The results of Charpy impact strength, tensile strength, and elongation at break for elastomer-compatibilized PPS/PA66 blends are summarized in Table II. Interestingly, the impact properties of the both nylon-rich PPS/PA66 polymer blends presented similar behavior with the addition of compatibilizer, that is, the impact strength first increased slowly with increasing concentration of both SEBS and

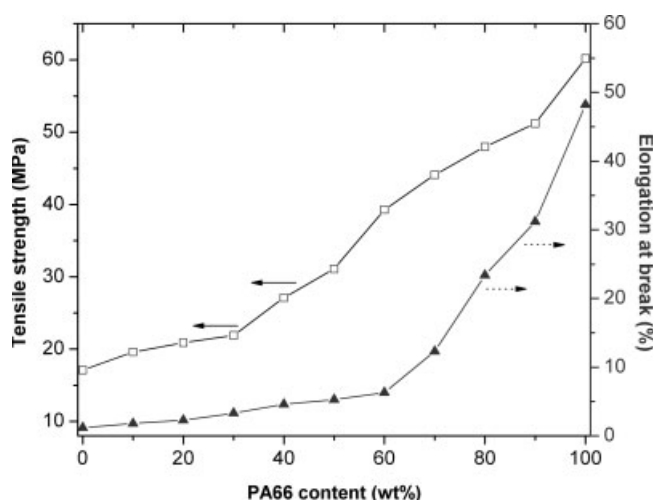


**Figure 3** Variation of tensile strength (□) and elongation at break (▲) with PA66 content for uncompatibilized PPS/PA66 blends.

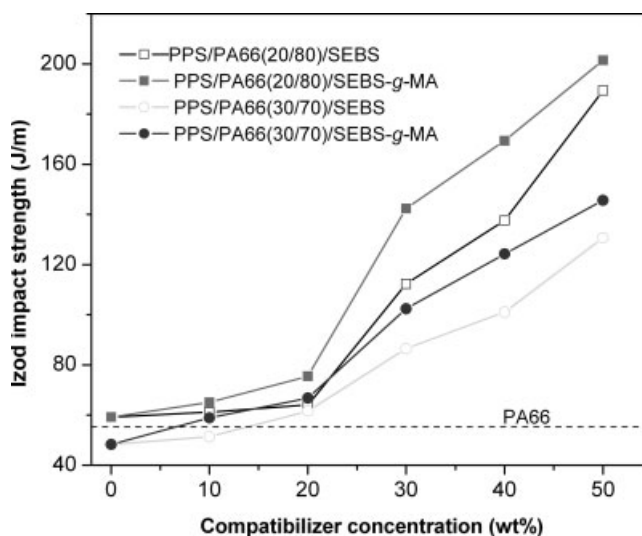


**Figure 4** Variation of Izod impact strength (left panel) and elongation at break (right panel) with compatibilizer concentration for PPS/PA66 (20/80)/SEBS (□), PPS/PA66 (20/80)/SEBS-g-MA (■), PPS/PA66 (30/70)/SEBS (△), and PPS/PA66 (30/70)/SEBS-g-MA (▲).

SEBS-g-MA up to 20 wt %, and then increased dramatically before the compatibilizer concentration reaching 30 wt %. The increase in impact strength slowed down when further increasing the concentration of compatibilizers. For example, when SEBS concentration increased from 20 to 30 wt %, a 75% improvement in Izod impact strength was achieved for PPS/PA66 (20/80) and 40% achieved for PPS/PA66 (30/70). For the SEBS-g-MA compatibilized blends, 89% and 68% improvement in Izod impact strength was observed for PPS/PA66 (20/80) and PPS/PA66 (30/70) blends, respectively. The brittle-tough transition<sup>20</sup> for our elastomer-toughened PPS/PA66 blends was achieved with the addition of ~ 20 wt % compatibilizer. The surface-to-surface interparticle distance,  $\tau$ , was estimated to be around 0.5  $\mu\text{m}$ .

Overall, SEBS-g-MA compatibilized PPS/PA66 polymer blends presented higher impact strength than SEBS compatibilized ones. The toughening effect is more significant in PPS/PA66 (20/80) blends. For example, by fixing the compatibilizer concentration at 30 wt %, SEBS-g-MA compatibilized PPS/PA66(20/80) blend (142 J/m) presented 27% higher impact strength than SEBS compatibilized one (112 J/m). For PPS/PA66 (30/70) blends, 30% improvement in impact strength was observed for SEBS-g-MA toughened blend (112 J/m) compared with SEBS toughened one (86.5 J/m).

It is worthy to note that the compatibilized PPS/PA66/elastomer blends were toughened with the addition of SEBS or SEBS-g-MA. With 20 or 30 wt % compatibilizer, nylon-rich PPS/PA66/elastomer tertiary blends presented tremendous improvement in impact strength in comparison with PPS/PA66

**TABLE II**  
**Effect of Compatibilizer Concentration on the Mechanical Properties of PPS/PA66**  
**Blends Compatibilized by SEBS and SEBS-g-MA**

Blends	Compatibilizer (wt %)	Charpy impact strength (kJ/m <sup>2</sup> )	Tensile strength (MPa)	Elongation at break (%)
PA66	0	4.8 ± 0.4	60.2 ± 0.61	48.2 ± 1.3
PPS	0	0.43 ± 0.02	17.1 ± 0.13	1.2 ± 0.1
PA66/SEBS-g-MA(80/20)	20	6.8 ± 0.1	32.9 ± 0.31	42 ± 0.9
PA66/SEBS-g-MA(70/30)	30	4.9 ± 0.2	29.5 ± 0.41	47 ± 1.2
PPS/PA66 (20/80)/SEBS	0	3.9 ± 0.2	46.3 ± 0.46	13.1 ± 0.4
	10	4.0 ± 0.1	37.5 ± 0.35	14.7 ± 0.7
	20	4.1 ± 0.3	33.1 ± 0.36	21.6 ± 1.0
	30	7.1 ± 0.6	28.3 ± 0.28	27.3 ± 1.3
	40	7.5 ± 0.8	23.9 ± 0.30	35.6 ± 1.2
	50	8.3 ± 0.6	22.5 ± 0.27	38.9 ± 1.7
PPS/PA66 (20/80)/SEBS-g-MA	10	4.1 ± 0.2	40.9 ± 0.32	18.9 ± 0.5
	20	4.5 ± 0.1	35.8 ± 0.41	24.0 ± 0.8
	30	7.9 ± 0.4	32.4 ± 0.42	31.2 ± 1.1
	40	8.8 ± 0.6	28.1 ± 0.56	37.6 ± 1.3
	50	9.3 ± 1.0	25.7 ± 0.64	41.2 ± 1.5
PPS/PA66 (30/70)/SEBS	0	3.3 ± 0.1	44.1 ± 1.21	12.3 ± 0.6
	10	3.5 ± 0.2	34.6 ± 1.06	13.6 ± 0.5
	20	3.6 ± 0.2	30.4 ± 1.02	19.9 ± 0.6
	30	4.3 ± 0.4	26.2 ± 0.96	25.2 ± 0.8
	40	4.9 ± 0.3	22.1 ± 0.89	31.4 ± 1.2
	50	6.7 ± 0.4	20.4 ± 0.84	33.6 ± 1.6
PPS/PA66 (30/70)/SEBS-g-MA	10	3.8 ± 0.2	38.6 ± 0.95	17.1 ± 0.9
	20	4.0 ± 0.6	33.8 ± 0.87	21.6 ± 1.1
	30	5.9 ± 0.3	30.4 ± 1.04	27.5 ± 1.2
	40	6.9 ± 0.5	26.8 ± 0.93	32.1 ± 1.6
	50	7.4 ± 0.8	24.9 ± 0.76	34.2 ± 2.1

binary blends. However, their impact strengths are a little bit lower than those of PA66/SEBS-g-MA (80/20 or 70/30) binary blends. Therefore, one can imagine that a part of the elastomer acts as an emulsifier, which exists in the interface of PPS and PA66 and reduces the interfacial tension between the two phases. Of course, most elastomers create a third domain in the PA66 matrix and act as impact modifiers. In this case, the nylon-rich blends are toughened when containing both rigid PPS particles and elastomer particles in ductile matrix. Similar behavior has been found in HDPE-rich PS/HDPE blends compatibilized by SEBS.<sup>21–23</sup> The ductility and toughness are improved as a result of the adequate differences in Young's modulus and Poisson's ratio between the brittle particles and polymer matrix, which induce compressive stress acting on the dispersed particles. Consequently, the deformation mechanism in dispersed particles may change from crazing to cold drawing because of the compressive stress.<sup>24</sup> It is noted that the SEBS and SEBS-g-MA played an important role in improving the toughness of nylon-rich blends. The presence of elastomer particles leads to improved interfacial adhesion between disperse phase and matrix and finer dispersion of rigid PPS and elastomer particles in nylon matrix.

The tensile strength of elastomer-toughened PPS/PA66 blends tends to decrease continuously with

increasing elastomer content, similar to those reported elastomer-toughened polymer blends.<sup>4,7–10,14</sup> However, the decrease in tensile strength is more obvious with the addition of SEBS compared with SEBS-g-MA. For instance, when 50 wt % elastomer was added, 51% and 44% loss in tensile strength was observed, respectively, for PPS/PA66/SEBS and PPS/PA66/SEBS-g-MA, in comparison with the uncompatibilized PPS/PA66(20/80) blends.

The variation of elongation at break with elastomer concentration is similar to that of Izod impact strength, that is, the elongation at break of elastomer toughened PPS/PA66 blends increased with elastomer concentration. However, SEBS-g-MA is more effective than SEBS in improving the ductility of PPS/PA66 blends.

### Fractography

The fracture surface can reveal the involved impact energy dissipation mechanisms upon impact testing. Figure 5 shows the SEM fractographs for uncompatibilized PPS/PA66 (90/10) and PPS/PA66 (50/50) blends. A large amount of irregular shaped PA66 particles (~ 1 μm size) are dispersed in PPS matrix. With increasing the content of PA66 to 50 wt %, the SEM micrograph changed from typical matrix-drop-let structure [Fig. 5(a)] to interlocking structure, with

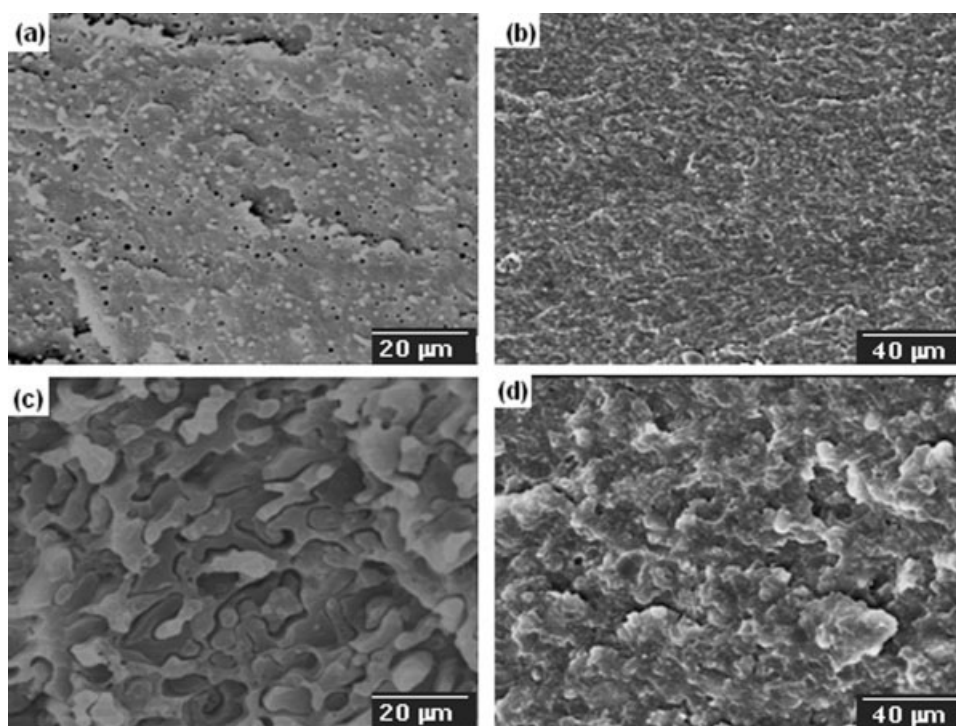


**Figure 5** SEM micrographs of impact-fractured surface of (a,b) PPS/PA66 (90/10) blend and (c,d) PPS/PA66 (50/50) blend. (a) and (c) beyond notch, cryogenically-fractured; (b) and (d) near notch, impact-fractured.

both PPS and PA66 as the continuous phase [Fig. 5(c)]. As indicated by the clear interface and weak interfacial adhesion [Fig. 5(a,c)], the compatibility between PPS and PA66 is poor. As a result, the fracture surface is very smooth, typical of a brittle failure. Similar morphology was also observed for the uncompatibilized PPS/PA66 (40/60) blend by Fu and coworkers.<sup>25</sup>

With the introduction of SEBS-g-MA, the interfacial adhesion between PPS and PA66 increased, as indicated by the obscure interface between dispersed phases and matrix [Fig. 6 (a,c,e)]. As mentioned above, only part of SEBS-g-MA acts as emulsifier and is located at the interface between PPS and PA66. Most ESI, however, created a third domain as tiny particles dispersed along with PPS particles in the nylon matrix. With increasing concentration of SEBS-g-MA, finer and more homogenous dispersion were observed for disperse particles [Fig. 6(a,c,e)]. As revealed from the morphology, a lot of large cavitations are readily observed in the fracture surface with the addition of SEBS-g-MA. When SEBS-g-MA concentration is increased to 20 wt %, the fracture surface changes remarkably and exhibits matrix shear yielding beyond the notch [Fig. 6(d)]. With further increasing SEBS-g-MA concentration to 30 wt %, the matrix yielding becomes more extensive and elongated matrix ligaments can be visible. Such fracture mechanism dissipates a significant amount of impact energy and thus, impact toughness is

improved remarkably. The toughening mechanisms occurring in various toughened and particle filled semicrystalline polymers were studied Kim and Michler<sup>26,27</sup> They pointed out that although void formation, followed by cavitations or debonding process, itself is a secondary factor contributing to toughness, it plays an important role for the activation of further plastic deformation of matrix materials during the micromechanical deformation process. Once the microvoid is formed in the matrix, the hydrostatic stress caused by stress concentration is released and the shear stress is lowered. The constrained conditions, that is, triaxial stresses, disappear, and the matrix behaves as if it was under plane stress conditions. Shear yielding deformations occur more readily under a biaxial stress state rather than the craze-favoring triaxial state. Now, it is generally believed that shear yielding of the matrix is the major energy-absorbing mechanism and therefore, the impact toughness is improved in this case [Fig. 6(d,f)].

Again, the degree of adhesion seems to increase with the introduction of SEBS-g-MA. The *in situ* formed PA66-co-SEBS-g-MA copolymer is believed to locate the interphase between PPS and PA66, which not only lowers their interfacial tension, but also suppresses the tendency of coalescence, thus resulting in a finer dispersion of PPS and also elastomer particles in matrix. For the former case, improved interfacial adhesion between the compo-

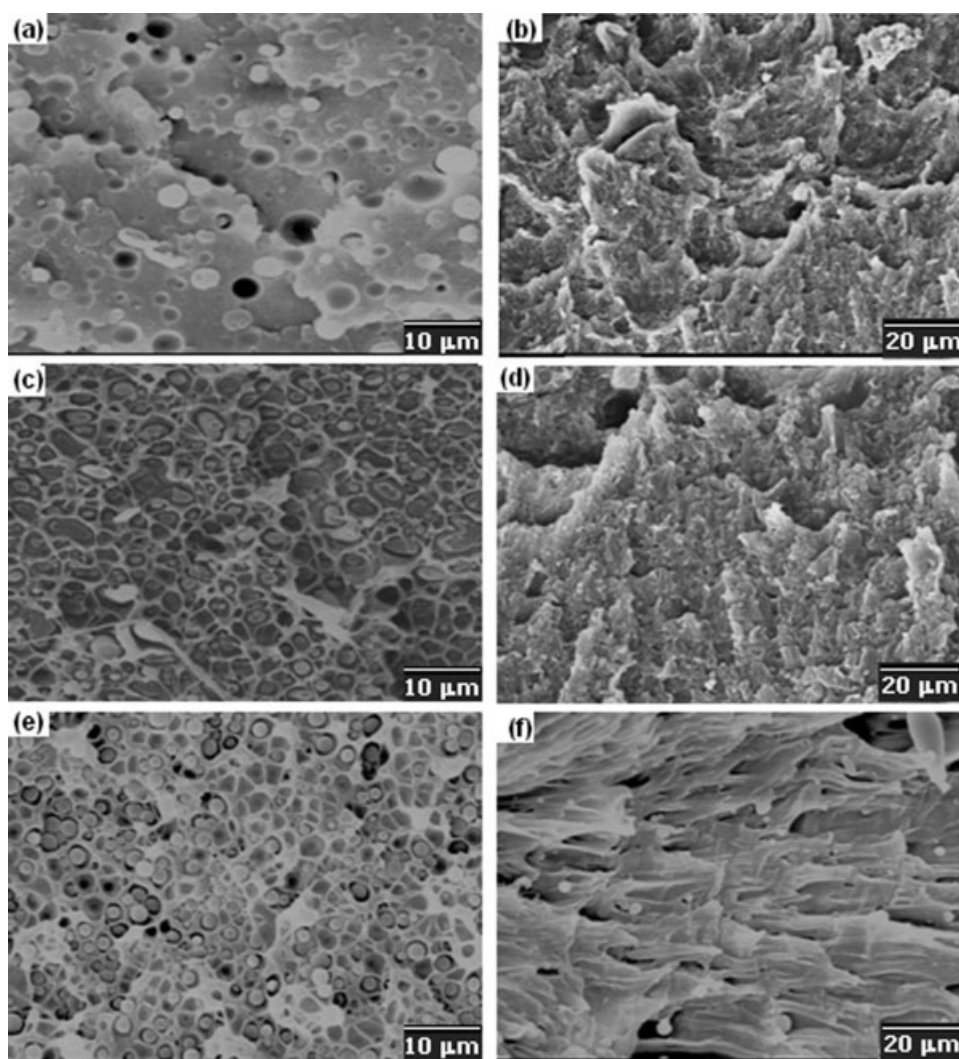


**Figure 6** SEM micrographs showing the fractured surface feature of PPS/PA66(20/80)/SEBS-g-MA blends containing: (a,b) 10 wt %; (c,d) 20 wt %; (e,f) 30 wt % SEBS-g-MA. (Left panel: beyond notch, cryogenically-fractured; right panel: near notch, impact-fractured).

nents can facilitate the stress transfer during impact fracture, which is demonstrated by fracture surface morphologies. For the latter one, finer and more homogenous dispersion of dispersed particles in continuous matrix can promote the formation of an interlocking structure in PPS/PA66 blends, which allows more equal sharing of imposed stresses and might therefore improve the mechanical properties of the blends.

### CONCLUSION

In this study, SEBS and maleic anhydride grafted SEBS were added into PPS/PA66 blends as interfacial modifier. The compatibilization efficiency of SEBS and SEBS-g-MA was investigated and compared in nylon-rich PPS/PA66 blends. Mechanical properties and fractography of uncompatibilized

PPS/PA66 and elastomer-toughened PPS/PA66 blends were investigated. SEM observations suggest that a fine dispersion and good interfacial adhesion were achieved with the addition of SEBS-g-MA. Mechanical properties demonstrated that the addition of elastomers considerably improved the toughness of PPS/PA66 blends. However, due to the *in situ* formation of SEBS interphase between PPS and PA66, SEBS-g-MA toughened PPS/PA66 blends provided better mechanical properties than SEBS-toughened ones. Impact-fracture morphology of PPS/PA66/SEBS-g-MA blends revealed that matrix shear yielding began to appear beyond the notch, when SEBS-g-MA concentration reaches 10 wt %. Further increasing of SEBS-g-MA concentration led to an extensive matrix yielding, which became the main mechanism of the impact energy dissipation upon impact testing.

## References

1. Jog, J. P.; Nadkarni, V. M. *J Appl Polym Sci* 1985, 30, 997.
2. Lopez, L. C.; Wilkes, G. L. *J Macromol Sci Chem Phys* 1989, 29, 83.
3. Geibel, J. F.; Campbell, R. W. In *Comprehensive Polymer Science*; Eastmond, G. C., Ledwith, A., Russo, S., Sigwalt, P., Eds.; Pergamon: Oxford, UK, 1989; Vol. 5, Chapter 32.
4. Masamoto, J.; Kubo, K. *Polym Eng Sci* 1996, 36, 265.
5. Kubo, K.; Masamoto, J. *J Appl Polym Sci* 2002, 86, 3030.
6. Kohan, M. *Nylon Plastics Handbook*; Hanser: New York, 1995.
7. Kubo, K.; Masamoto, J. *Kobunshi Ronbunshu* 1999, 56, 426.
8. Nam, J.-D.; Kim, J.; Lee, S.; Lee, Y.; Park, C. *J Appl Polym Sci* 2003, 87, 661.
9. Hisamatsu, T.; Ishikawa, Y. *Polym Preprint Jpn* 1998, 47, 2765.
10. Hisamatsu, T.; Nakano, S.; Adachi, T.; Ishikawa, M.; Iwakura, K. *Polymer* 2000, 41, 4803.
11. Ishikawa, M. *Kobunshi Ronbunshu* 1990, 47, 83.
12. Ishikawa, M.; Chiba, I. *Polymer* 1990, 31, 1233.
13. Ishikawa, M. *Polymer* 1995, 36, 2203.
14. Tjong, S. C.; Xu, S. A. *J Appl Polym Sci* 1998, 68, 1099.
15. Koo, K. K.; Inoue, T.; Miyasaka, K. *Polym Eng Sci* 1985, 25, 741.
16. Chen, Z.; Liu, X.; Li, T.; Lü, R. *J Appl Polym Sci* 2006, 101, 969.
17. Chen, Z.; Liu, X.; Lü, R.; Li, T. *J Appl Polym Sci* 2006, 102, 523.
18. Lu, M.; Keskkula, H.; Paul, D. R. *J Appl Polym Sci* 1995, 58, 1175.
19. Wu, D.; Wang, X.; Jin, R. *J Appl Polym Sci* 2006, 99, 3336.
20. Wu, S. H. *Polymer* 1985, 26, 1855.
21. Bureau, M. N.; Kadi, H. E.; Denault, J.; Dickson, J. I. *Polym Eng Sci* 1997, 37, 377.
22. Tjong, S. C.; Xu, S. A. *J Appl Polym Sci* 1998, 68, 1099.
23. Tjong, S. C.; Xu, S. A. *Polymer* 2000, 32, 208.
24. Kurachi, T.; Ohta, T. *J Mater Sci* 1984, 19, 1699.
25. Zou, H.; Zhang, Q.; Tan, H.; Wang, K.; Fu, Q. *Polymer* 2006, 47, 6.
26. Kim, G. M.; Michler, G. H. *Polymer* 1998, 39, 5689.
27. Kim, G. M.; Michler, G. H. *Polymer* 1998, 39, 5699.